Research papers

Catchment-scale hydrology simulations using inter-variable multi-parameter terrain descriptions

Bastian van den Bout*, Victor Jetten

University of Twente, ITC, Earth System Analysis, Europe

ABSTRACT

Global simulations of hydrology and hydraulics combine network-type routing with hydrological simulations on large Hydrological Response Units (HRUs). In order to efficiently simulate the hydrological response of HRUs, empirical equations are generally applied to averaged physical parameters or empirical constants. The usage of physically-based equations on a spatial description of the HRU could provide benefits in accuracy and scenario assessment. In this research we develop a multi-parameter inter-variable terrain description to simulate HRU hydrology and flow. Water is distributed over these classifications and used for application of physically-based equations. A mass-balanced scheme is presented that uses parameter inter-variability matrices to update the distributions of water. Furthermore, the method is used to simulate processes using physically-based equations that result in fluxes from and to other classes within a distribution, resulting in a semi-spatial process description within an HRU. Finally, physically-based equations are thus applied to a dynamic semi-spatial HRU description using multiple inter-variable physical parameters. A variety of study cases on hypothetical and real events are performed to highlight the behavior and sensitivity of the model, as well as comparison to existing methods. Uncalibrated comparison with full spatial flow simulations show reasonable agreement with a Nash-Sutcliffe coefficient of 0.47. Comparison to simulations of real events on catchments in Northern China and Central Spain show good comparability with an average Nash-Sutcliffe coefficient of 0.56. The performance of the model indicates good applicability when considering the efficiency of the method. Simulation time is in the ranges from fractions of seconds on consumer hardware without dependency of the area of the catchment. Additionally, the model uses physical parameters as input and physically-based descriptions of processes. This results in interactions between infiltration and flow that alter flow dynamics and hydrograph shapes in similar manners to full spatial hydrology and flow models. Finally, the method provides the possibility of linked additional processes such as groundwater and erosion, and could be applied on a global scale.

1. Introduction

In solving the massive global and local challenges in the availability of clean water, global or regional-scale hydrological models are frequently used. Such models require the simulation of land surface hydrology and flow routing (Bierkens et al., 2015). Flow routing is typically approximated by simulating kinematic water flow over a fixed river network similar to a local drainage direction network. Between these one-dimensional river sections, there exists Hydrological Response Unit (HRU) of which the outflow feeds the channel network. The simulation of a water balance within these HRUs requires partitioning of rainfall (and snowmelt) into infiltration, runoff, evapotranspiration and other storages and fluxes (De Graaf et al., 2015). Based on these fluxes, important variables such as the soil water content and are

determined. Finally, runoff and river flow can lead to global flood predictions (Yamazaki et al., 2014), raise awareness and estimate the influence of climate change (Hirabayashi et al., 2013).

Simulating the hydraulic response of HRU's for global application is a challenging process. The HRU's can be divided into regular squares through rasterization, or polygons using other criteria to set boundaries (Flügel, 1995). For larger HRU's, direct spatial application of physically-based equations demands both data accuracy, computational capacity and time, often beyond what is possible. This leads to usage of a simplified description of the terrain within simulations (Arnold et al., 2012). For example, several existing approaches take averages for important hydrological parameters of soil or surface (Soil Conservation Service, 1972; Morgan, 2001). However, processes are non-linear and therefore the application of a function to a spatial average does not

have to be equal to the spatial average of the applied function. Other approaches reduce the need for these parameters and capture the behavior of the HRU in empirical parameters that can be obtained through calibration (de Graaf et al., 2015).

Several methods exist for non-spatial modelling of discharge from an HRU. The curve number method uses an empirical relationship that estimates the fraction of water and has been developed and maintained by the soil conservation service in the U.S.A. (Soil Conservation Service, 1972). The curve number can be used to replace the cruder runoff coefficient in the rational method. Furthermore, if unit hydrographs are available, and a time of concentration is estimated, a full hydrograph can be estimated (e.g. TR-55 method). The Morgan-Morgan-Finey (MMF) model uses an empirical equation based on theoretical considerations (Morgan, 2001; Morgan and Duzant, 2008). The model proposes a negative exponential curve can be used to predict the quantity of infiltration out of the total rainfall during a specific time-period (typically a day). Shresta and Jetten (2018) adopted this equation to a daily spatial water balance, replacing the numerator with the daily soil moisture deficit of the control zone and the denominator with the daily rainfall. The rational method estimates peak flow based on steady state assumptions between incoming rainfall intensity and out-going discharge (Kuichling, 1889; Thompson, 2006; Hayes and Young, 2006). Due to this assumption it is meant to be applied to small-scale drainage areas such as sewer systems. The effect of infiltration is then compensated by a constant runoff coefficient, which distributes water over infiltration and runoff generation. The ARNO scheme and Improved ARNO scheme are types of "bucket" hydrology schemes (Dümenil and Todini, 1992; Hagemann and Gates, 2003). Here, the soil water capacity of a larger area is modelled as a large collection of smaller containers or soil water capacities. This distribution is generally taken as a power law. In practice, any non-infiltrated water is released as discharge from the simulated area. This type of model is frequently used in global hydrological models (De Graaf et al., 2015). Single linear reservoir models have been used in a variety of models (Crawford and Linsley, 1966; James, 1970; Foroud, 1978). The linear reservoir method simplifies the complex flow patterns of a catchment by envisioning a sequence of linearly reacting storage reservoirs (López et al., 2005). Each reservoir is located at lower elevation, closer to the outlet of the area. The outflow rate for a reservoir is linearly dependent on the total storage within that specific reservoir. Due to the linearity of the reservoirs and the linking, there is, in this approximation, a spatial distribution of water over the catchment. Furthermore, the outflow of this method is time-dependent and resembles the typical wave shapes of hydrographs

Empirical formulations of a HRU response often benefit from their computational simplicity and ability to run on large and low-resolution datasets. Values for empirical parameters are frequently obtained by means of calibration and validation. This method of estimating parameters can also be a downside as it does not allow for estimation of parameters for future scenarios or based on direct measurements. In contrast, the usage of physical parameters allows for direct assessment from measurement, and estimation of parameters for alternative scenarios. By inputting alternative scenarios, impact and consequences from processes such as climate change, land use change or urban growth can be assessed. However, for the benefits of physically-based parameters to be used, a more complex description of the terrain and subsurface of a HRU. This would increase computational cost beyond the limitations of current equipment. Current attempts in modelling that go beyond a HRU averaging include the linear reservoir method (Crawford and Linsley, 1966), which has not been applied to a global scale. This method describes the terrain based on distribution of a single parameter, in this case elevation. Other approaches to this use single parameter distribution for other parameters related to the soil (Hagemann & Gates, 2003). However, in these cases, inter-parameter variability is not taken into account and the selected parameters are taken as independently varying. In reality, many parameters are causally connected and therefore correlated.

The objective of this work is the development of a method that can efficiently simulate hydrology using a physically-based process description. A new method is explored to simulate clumped semi-spatial hydrology and flow from HRUs by using multi-parameter inter-variable terrain descriptions. The concept of semi-spatial discretization for hydrology is extended to physically-based equations. In section 2, we develop the mathematical framework for the semi-spatial discretization of multi-parameter inter-variable terrain. Afterwards, we implement in this framework precipitation, infiltration and surface flow based on physically-based equations. In section 3, we apply the developed method to real-world cases and several numerical studies. Finally, in section 4, we discuss the implications and requirements of the scheme, and how these impact its possible application.

2. Model development

2.1. Multi-parameter catchment classification

Similar to Crawford and Linsley (1966) and Hagemann & Gates (2003) a semi-spatial classification of the terrain is performed. In contrast with these authors, the presented derivation uses a classification of multiple parameters. We define the parameters $X^1, .., X^n, .., X^N$ with N the number of parameters. For parameter one, classes are notated as $X_1^1, .., X_i^1, .., X_C^1$ with C the number of classes. These classes can be chosen to have an equal surface area within the HRU, but could be chosen in other manners such as based on existing land use classifications. In this section, we use three parameters as example, land use, slope and soil, each discretized into four classes (Fig. 1). These parameters are not direct input for the model, but represent a choice of physical parameter. In section 2.5, the actual implementation of the physically-based equations will determine the actual physical parameters that are classified.

For each terrain parameter, the classes represent planar surface that can store and exchange water. In each of the classes, the surface area is denoted $A(X_i)$. Note that the total area for each of the parameters, the sum of the area for each class, is equal to the total surface area of the HRU (Equation (1)).

$$\sum_{i=0}^{C} A(X_i^n) = HRU\ area \tag{1}$$

where X_i^n is a specific discretized parameter class (superscript indicates parameter, subscript indicates class) Sampling a random point within the HRU, the probability of finding, for example, a specific land use class can be expressed probabilistically based on the relative frequency of the class (Equation (2)).

$$P(X_i^n) = \frac{A(X_i^n)}{A(HRU)} \tag{2}$$

where $P(X_i^n)$ is the probability that for a specific parameter n (land use for example), at a random location, class i is found.

For each of the parameters, each class represents a surface plane that holds some volume of water, defined as $V(X_i^n)$. If the terrain experiences a homogeneous precipitation (homogeneous influx of water), the volumes for each of the classes increases by the rainfall volume multiplied by the probability of the specific class.

$$\Delta V(X_i^n) = R \cdot P(X_i^n) \tag{3}$$

where R is the rainfall volume and $\Delta V(X_i^n)$ is the fluid volume change for parameter n and class i.

We employ the following terminology: the fluid volumes in the classes for a parameter represent the distribution of water over that parameter (Fig. 1). By combining 1 and 3, it can be found that the total volume of water distributed over the classes of each parameter is equal (Equation (4)). For a mass-conserving simulation, this must remain so for any operation performed on the fluid volumes.
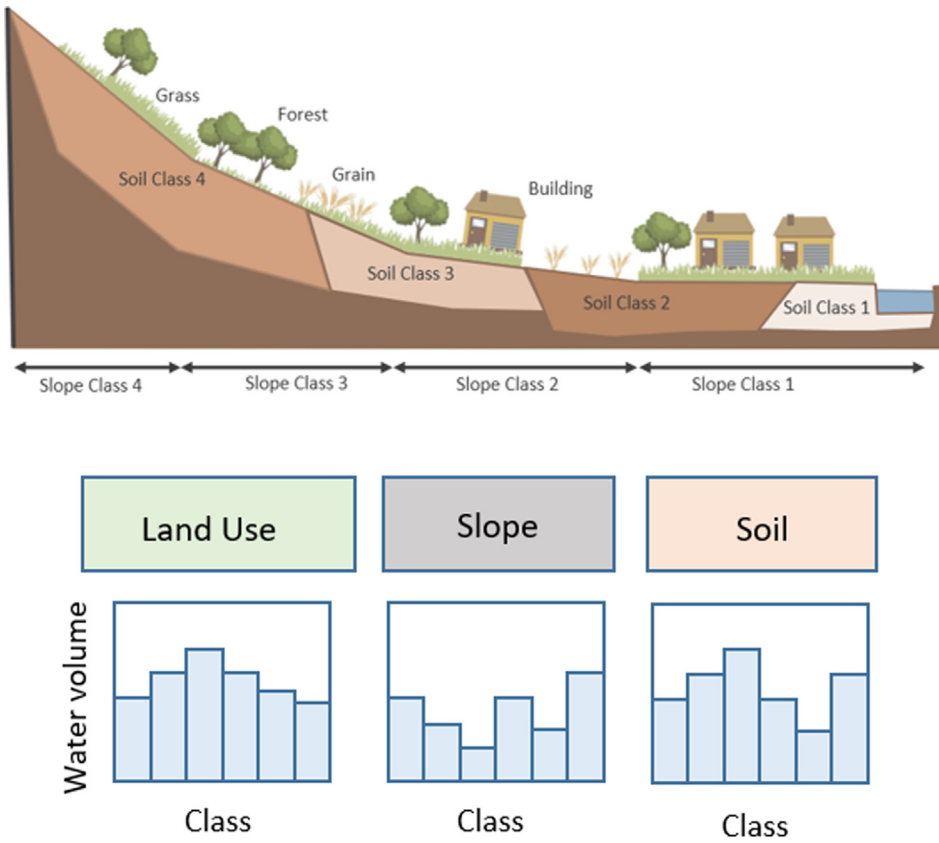
Fig. 1. Catchment discretization into three physical characteristics (soil type, land cover types and slope). . Water on the surface is distributed over the classified parameters. In the example of this figure, if all surface water is contained in soil class 1, the water is distributed over urban and grass land use classes and the lowest slope class. The distributions are thus generally not equal, but contain identical total water volumes.

$$\sum_{i=0}^{C} \sum_{n=0}^{N} V(X_i^n) = V_{total} \tag{4}$$

where V_{total} is the total fluid volume on the HRU terrain surface.

2.2. Multi-parameter inter-class probability

While precipitation acts homogeneously on the water distributions, this is not the case for other processes. Other processes can act in higher or lower degree for distinct classes of physical parameters. For example, soil types influence infiltration, and specific soil classes might lose a relatively higher volume of water due to this process. We define a fluid volume flux Q_i^n with i from 0 to C, which acts on a water distribution to change the volumes $\Delta V(X_i^n) = Q_i^n$. Since we require the water distribution for each parameter to be consistent and of identical total volume, there must be a flux for the other distributions. We must therefore define a manner in which we can remove water from a specific class, but maintain mass conservation and consistency with the other water distributions.

To do so, we define the inter-class probability matrix $P(X_i^n, X_j^k)$ which indicates the probability that for an area containing class i for parameter n, it has class j for parameter k (Fig. 2). This probability is equal to the normalized fractional area of class i for parameter n and class j for parameter k (Equation (5)).

$$P(X_i^n, X_j^k) = \frac{A(X_i^n, X_j^k)}{\sum_{l=0}^{C} A(X_i^n, X_l^k)} \tag{5}$$

Normalization is required since there must be a probability of 1 that there is some class for parameter $K \cdot \left(\sum_{l=0}^{C} P(X_i^n, X_l^k) = 1 \right)$.

2.3. Mass conserving flux transfer

Using the inter-class probability, a flux transformation can be defined that transforms a flux from classified parameter space of one
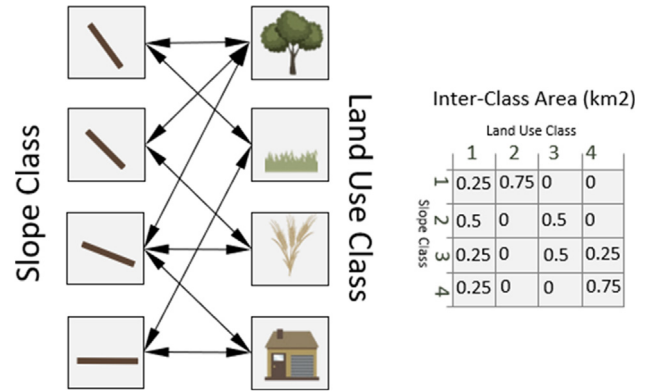

Fig. 2. The probabilities of combinations of classes existing can be identified in the inter-class matrix.

parameter to the space of a second parameter. This transformed flux can then be used to alter fluid volumes in the water distribution over the second parameter. We assume here that the flux transforms according to the product of its inter-class probability and normalized fractional water content (Equation (6)).

$$Q_j^k = \sum_{i=0}^{C} Q_i^n \cdot \frac{P(X_i^n, X_j^k) \cdot V(X_j^k)}{\sum_{l=0}^{C} P(X_i^n, X_l^k) \cdot V(X_l^k)} \tag{6}$$

In practical terms, equation (6) defines the estimation of the exact distribution of water over the full terrain in a probabilistic manner. It is important to verify the conservation of mass in this transformation. The sum of transformed fluxes is required to be equal to the sum of the original fluxes $\left(\sum_{i=0}^{C} Q_i^n = \sum_{i=0}^{C} Q_i^k \right)$. This can be shown due to $\sum_{i=0}^{C} \frac{P(X_i^n, X_j^k) \cdot V(X_j^k)}{\sum_{l=0}^{C} P(X_i^n, X_l^k) \cdot V(X_l^k)} = 1$ and switching the double summation.
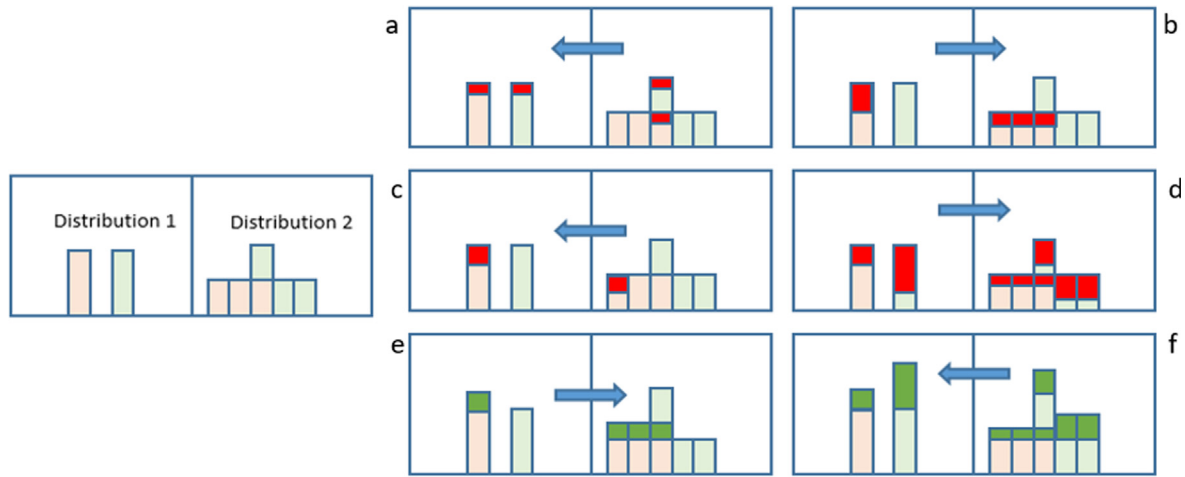
Fig. 3. Several typical types of flux transformation for both subtractive flux (negative, red, e.g: infiltration removing surface water) and additive (positive, green, precipitation adding surface water). The blue arrow indicates the direction of the flux transform. In order to obtain a mass-balanced and consistent distribution of water, it is assumed that a mixed volumes scale linearly to their originating distribution. (For interpretation of the references to colour in this figure legend, the reader is referred to the web version of this article.)

The proposed transformation rule provides the required properties: mass conservation, volume positivity and adressing inter-class areas and parameter intervariable water distributions (see Fig. 3 for examples of flux transformations).

For each combination of classes, an area $A(X_i^n, X_j^k)$ is defined. For each individual parameter class, a surface area and flow volume area known ($A(X_i^n)$ and $V(X_i^n)$). In order to implement processes, a water volume for a combination of classes ($V(X_i^n, X_j^k)$) is required. Using the same principle used above for flux transfer, the water volume on a combination of parameter classes can be defined (Equation (7)).

$$V(X_i^n, X_j^k) = V(X_i^n) \cdot \frac{P(X_i^n, X_j^k) \cdot V(X_j^k)}{\sum_{l=0}^{C} P(X_i^n, X_l^k) \cdot V(X_l^k)} \tag{7}$$

where $V(X_i^n, X_j^k)$ volume of fluid present on the surface area $A(X_i^n, X_j^k)$. The combination of these variables defines the fluid height on the surface $H(X_i^n, X_j^k) = \frac{V(X_i^n, X_j^k)}{A(X_i^n, X_j^k)}$.

2.4. Flow processes

We have defined a flux transformation based on the inter-class probabilities. A similar approach can be taken to simulate flow-processes in a semi-spatial manner. First, this requires the surface slope as a parameter to be classified. Changes in the water volume within a class then depend on the probability of outflow P_S (Equation (8)).

$$\Delta V(X_i^{slope}) = \sum_{j=0}^{C} Q_{out}(X_j^{slope}) \cdot P_S(X_j^{slope}, X_i^{slope}) \tag{8}$$

where $Q_{out}(X_j^{slope})$ is the outgoing discharge from the surface plane element described by slope class j and $P_S(X_j^{slope}, X_i^{slope})$ is the probability that a volume of water leaving an area with slope class j enters slope class i.

This will represent the terrain in terms of a cascade of sloping planes, where water is re-distributed over the slope classes by using a semi-spatial probabilistic expression of the terrain.

In order to obtain an expression for Q_{out} and P_S, slope map for the HRU is rasterized into regular rectangular elements of size Δx. Afterwards, a drainage network is calculated using a local drainage direction with pit removal algorithm. The spatial inter-class probability P_S can now be estimated by means of counting the frequency of slope classes in direct downslope neighbors (Equation (9)).

$$P_S(X_j^{slope}, X_i^{slope}) = \frac{A(X_i^{slope} \text{ directly downslope neighbor of } X_j^{slope})}{A(X_j^{slope})} \tag{9}$$

Equations (9) and (5) are analogous, as they use frequency for probability estimationFor a given timestep Δt, Q_{out} can similarly be expressed based on the rasterized slope of the HRU (Equation (10)).

$$Q_{out}(X_j^{slope}) = V(X_j^{slope}) \Delta \frac{\Delta t \cdot v(X_j^{slope})}{\Delta x} \tag{10}$$

where $v(X_j^{slope})$ is the velocity of the fluids stored in slope class j.

A schematic overview of the proposed flow scheme is shown in Fig. 4.

2.5. HRU outflow

Besides internal flow within a HRU, outflow exists where fluids enter a river or channel network that acts as an outlet. In one of the slope classes (typically the most gentle slope) an outlet may occur. Here, a part of the estimated discharge is not re-distributed among the slope classes, but instead counted as outgoing discharge through the outlet. Similar to the semi-spatial flow scheme, the probability of HRU
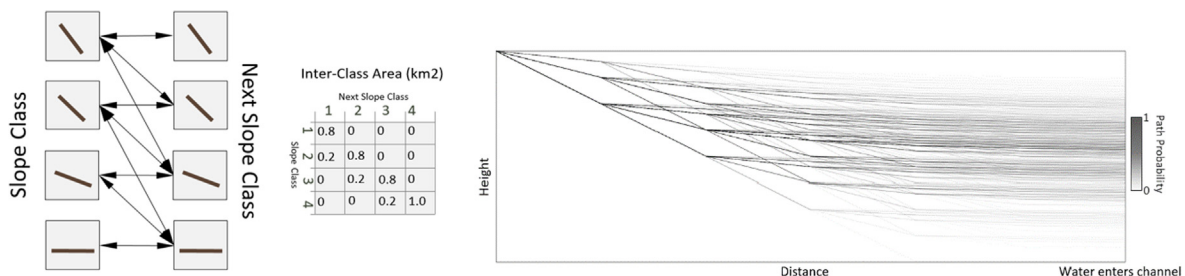
Fig. 4. All possible sequences of slopes that result in a water particle flowing to the outlet at elevation 0. Each path has unique probabilities within a catchment.
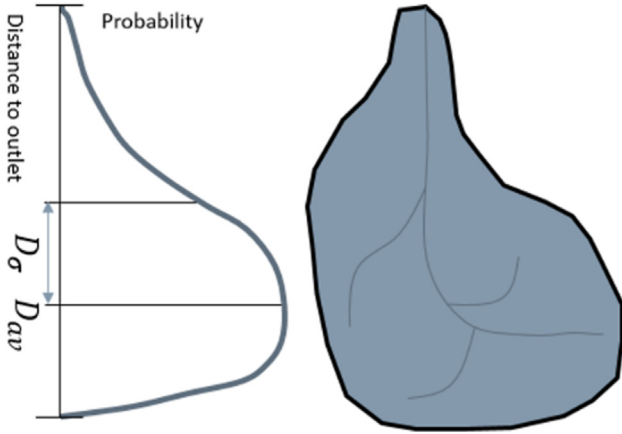
Fig. 5. The probability distribution of the distance to outlet can be approximated by using the average distance and variance of the distance to outlet.

outflow for each slope class (P_{out}) can be defined. Given this probability, the outflow can then be estimated (Equation (11)).

$$Q_{outflow}(X_j^{slope}) = Q_{out}(X_j^{slope})\Delta P_{out}(X_j^{slope}) \tag{11}$$

To accurately estimate fraction of discharge flowing through the outlet, we utilize a probabilistic approach to catchment shapes. In any catchment, the distance from each location towards the outlet is distributed between zero and the furthest location (Fig. 5)

In the example give, and in many characteristically tree-shaped catchment, there is a slow rise in outflow probability with increasing distance. Due to the branching, tree-like, nature of watersheds, the distribution of distances to the outlet often features asignificant peak beyond half the full length of the watershed. Using a geographic information system to create a drainage network, both the average and the square root of the variance of the 'distance to outlet' can be obtained. Using these, we estimate the fraction of water that, given a cumulative average travel distance, is at or further then the outlet (Fig. 6).

Since a full distribution of the distances to outlets are unknown, this is approximated using an existing probability density function. This function is parameterized using the average distance to outlet and the variance (D_{av} and D_σ) values. In the examples provided in this research, a Weibull distribution is used due to its similarity to the expected
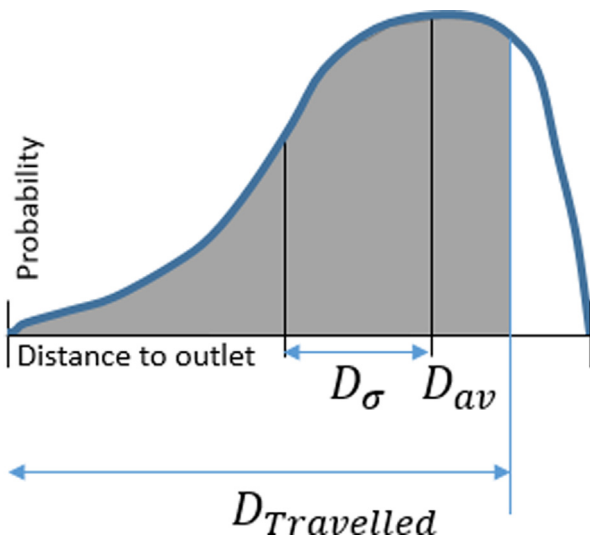

Fig. 6. With increasing average travelled distance, the probability of flow being directed outward of the catchment increases according to the cumulative distribution.

characteristic distributions of catchments, its flexibility in shapes, limited parameters, and the fact that it only assigns probability to positive values.

To define P_{out}, the distance travelled by the fluid volume is defined (D). The travelled distance for the fluid volumes on the slopes can expressed as (Equation (12)).

$$\frac{\Delta(V(X_i^{slope})\Delta D(X_i^{slope}))}{\Delta t} =$$

$$\Delta t \Delta v(X_i^{slope}) + \sum_{j=0}^{C} Q_{out}(X_j^{slope})\Delta P_S(X_j^{slope}, X_i^{slope})\Delta D(X_j^{slope}) \tag{12}$$

where $D(X_j^{slope})$ is the distance travelled on average by the fluid volume in slope class j.

Equation (12) is analogous to momentum conservation in finite difference schemes. In addition to incrementing travelled distance by the velocity during a timestep, travelled distance as a property of the fluids is conserved.

2.6. Modelling infiltration and runoff generation processes using physically-based equations

Using the mathematical framework provided in the previous sections, hydrological processes can be implemented. Here, precipitation, infiltration and runoff are implemented to describe a simple HRU response.

Precipitation results in water being added homogeneously to the water distributions. After the addition of rainfall to the surface, the primary process of the simulation is overland flow as estimated by Mannings surface flow equation (Equation (13)) (Maidment, 1993).

$$v = \frac{1}{n}\sqrt{s} R^{\frac{2}{3}} \tag{13}$$

where n is Mannings surface roughness coefficient, s is the slope and R is the hydraulic radius (defined for shallow flows to be approximately equal to the flow height).

The Green and Ampt infiltration model is implemented for infiltration (Green and Ampt, 1911). This model assumes a wetting front moving down into the soil due to infiltrating rainfall. The resulting potential infiltration is subtracted from the available surface water (Equation (14)).

$$f_{pot} = -K_s\left(\psi\frac{\theta_s - \theta_i}{F} + 1\right) \tag{14}$$

Where f_{pot} is the potential infiltration rate (ms^{-1}), F is the cumulative infiltrated water (m), θs is the porosity ($m^3 m^{-3}$), θ_t is the initial soil moisture content ($m^3 m^{-3}$), ψ is the matric pressure at the wetting front ($h = \psi + Z$) (m) and K_s is the saturated conductivity (ms^{-1}).

The input parameters for the model can now be determined based on the required input for the equations. Flow requires only Mannings surface roughness coefficient. Land use is therefore classified based on this parameter. In contrast to flow, infiltration requires four parameters, saturated conductivity, matric suction, initial moisture and the saturation moisture level. We choose to classify one of these, saturated conductivity. This maintains the simplicity and efficiency of the model. The remaining parameters required for infiltration are obtained by averaging within the area of a class for saturated conductivity.

After parameter selection, processes must be implemented. There are several options to simulate a process. The first option is to calculate fluxes for each combination of each parameter. This increases computational costs, but allows for more detailed description of behavior given different combinations of the physical parameters (Equation (15)).

$$\bar{I}(X_i^{ksat}) = \sum_{j=0}^{C} \sum_{k=0}^{C} I(X_i^{ksat}, X_j^{slope}, X_k^{land\ use}) \tag{15}$$

where $\bar{I}(X_i^{ksat})$ is the average infiltration for the area represented by
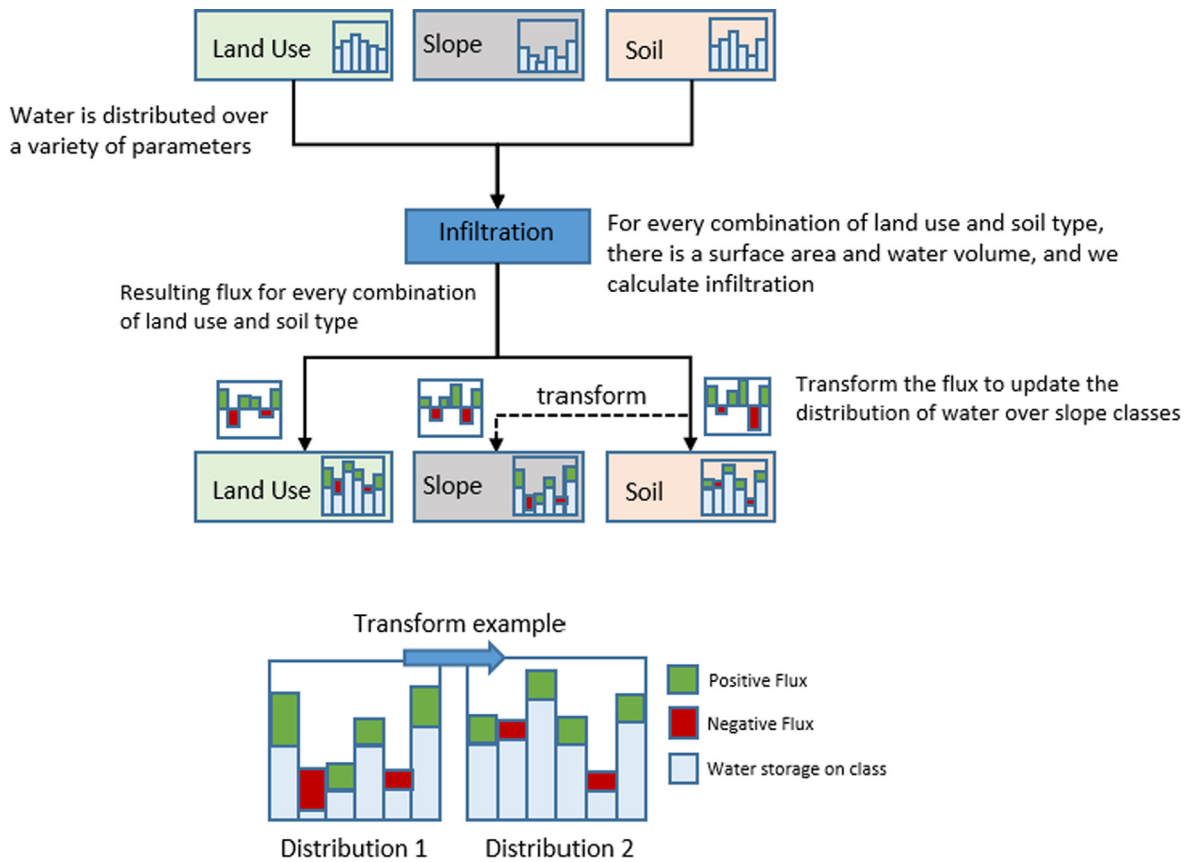
Fig. 7. (top) We simulate a process for each combination of the relevant classified parameters. Resulting flux is calculated for those same parameters. To update water distribution over other classified parameters, a flux must be transformed. (bottom) An example of a flux transformation.

class i of hydraulic conductivity.

In practice, the increased computational cost coming from the double summation prevents efficient implementation of equation (14). The second option, which is chosen in this work, is to simulate a process only for each combination of relevant parameters. For example, in infiltration models, slope is generally ignored since its value does not directly alter infiltration (Mishra et al., 2003). Thus, infiltration can be simulated using the distribution of water over soil types and land use types (Equation (16))

$$\bar{I}(X_i^{ksat}) = \sum_{k=0}^{C} I(X_i^{ksat}, X_j^{\bar{slope}}, X_k^{land\ use}) \tag{16}$$

Afterwards, the volume flux is known for land use and soil type classes. Additionally, the volume flux is required for the remaining parameter. The transformation rule in equation (5) can be used to obtain this. An example of the implementation of infiltration is provided in Fig. 7.

2.7. Model input parameters

The final model setup is shown in Fig. 8.

The model requires a classification of slope, land use and soil. For land use, Manning's surface roughness coefficient is classified. For soil, the saturated conductivity is classified. In addition, soil classes are provided an average value for saturation soil moisture and matric suction. Thus, the model requires spatial input for five physical parameters, and a timeseries of precipitation (Table 1).

An initial preparation step is required where a drainage network is calculated for the HRU. From this, the D_σ and D_{av} are required, as well as the inter-slope probability values. These calculations can be efficiently performed in a GIS-script as an initial calculation and do not

need to be repeated for each simulation.

3. Model application

In this section, several applications of the proposed method will be shown. A set of both hypothetical and real catchments are simulated and compared with results from fully spatially distributed simulations of overland flow and infiltration.

3.1. Numerical tests

Several catchments have been generated to test the proposed method. Generation was done using a fractal-type branching tree with a variety of angles and skewness. Finally, based on the distance from the tree network, an elevation model as created using 10 m gridcells (Fig. 9). Physical parameters for the areas are homogeneous, and set as $\{K_s, \psi, n, \theta_i \theta_s\} = \left\{10\frac{mm}{h}, 10cm, 0 \times 1, 0 \times 4, 0 \times 5\right\}$. For these areas, we run a full spatial surface flow model, OpenLISEM, using a kinematic wave flow approximation (Bout and Jetten, 2018).

3.1.1. Results

The simulation results for the hypothetical catchments, together with fully spatial kinematic wave simulations, and used rainfall intensities, are shown in Fig. 10.

In general, the proposed method captures outflow behavior similar to the full spatial simulations of the catchments. The averaged performance of the model, without calibration, is $R^2 = 0.47$. While calibrated models typically reach higher values, it is important to evaluate the performance in light of the relatively simple, non-spatial setup of the model. Additionally, no calibration was performed. The outputs thus indicate that the method can provide reasonable simulations of
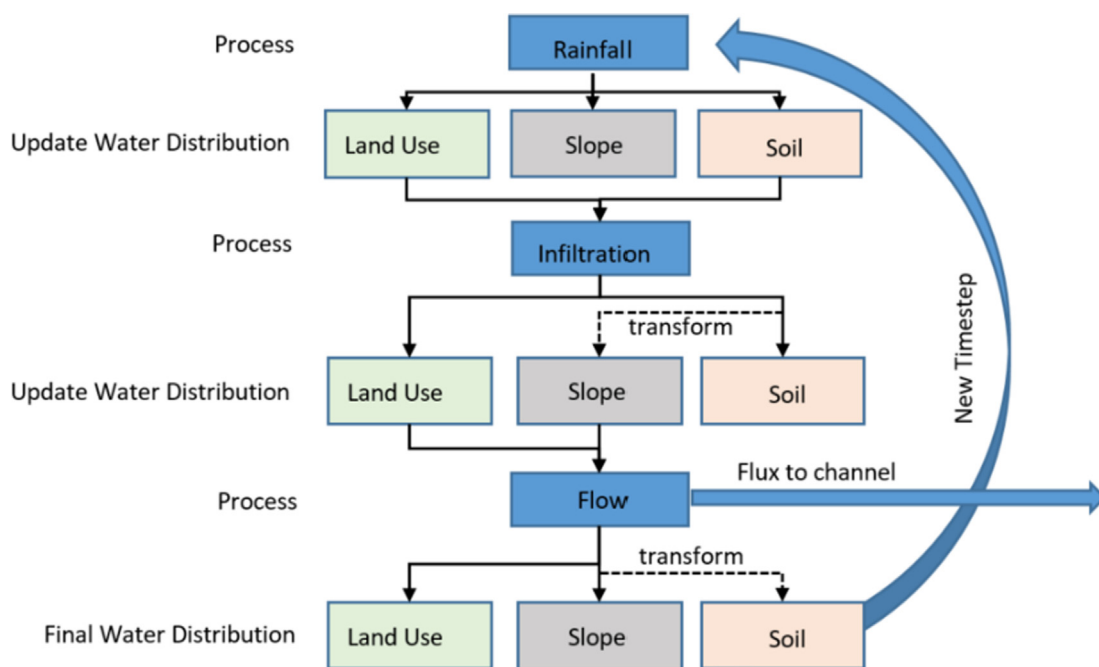
Fig. 8. A final flowchart for the proposed methodology. Processes are blue and required flux transforms are indicated. The spatial routing scheme is part of the flow process. (For interpretation of the references to colour in this figure legend, the reader is referred to the web version of this article.)

hydraulic response without the need for full spatial simulation. Additionally, the shape and topography influences the outputs in a realistic manner. Hydrograph peak height, width and shape are altered in ways similar to the full spatial flow model.

For several other aspects, the proposed method lacks detail when compared to the fully spatial simulations. In particular, the sudden arrival shown by the third and fourth catchment is not captured well by the model. Part of the cause of this is the relatively small variance in distance to outlet, which leads to a small wave, where water arrives simultaneously. Though this type of behavior is estimated in the proposed method, it is in these cases underestimated, possibly due to the extreme catchment shapes. For the first and second catchments, the behavior difference due to the distribution of the distances to the outlet are significantly better predicted. These types of catchment shapes are also more alike to naturally occurring watersheds.

3.2. Real study cases

We apply the proposed method to two real catchments, the Danandou and Prado areas (Fig. 11. and Fig. 12.). The first of these is the Danandou catchment, a rural area in the Loess plateau in China, which was previously used by Hessel et al. (2003, see also Hessel et al., 2003b; Hessel & van Asch, 2003 and Hessel and Jetten, 2007) to calibrate a previous version of the LISEM model. This 257 ha region is characterized by steep slopes (> 20°) , and dry non-vegetated terrain.

For this catchment three precipitation events from 20 to 07-1999, 23–08-1998 and 01–08-1998 will be used. Together with measured rainfall intensity, discharge after these events is available for every two minutes. The spatial resolution of this dataset is 10 m.

A second catchment in Prado, South-Eastern Spain, will be used. This 50 km^2 semi-arid region is predominantly covered by dry shrubs and forest and has previously been used with LISEM by Baartmans et al. (2013, see also Baartmans et al., 2012a; Baartmans et al., 2012b). Both rainfall and discharge data are available for three rainfall events. The spatial resolution of this dataset is 20 m.

Calibration occurs by altering the values of the saturated conductivity and Mannings surface roughness with a homogeneous multiplier. The simulations were performed for a total of 100 combinations of input, with the multipliers ranging between 0.5 and 1.5. Model accuracy was assessed based on the Nash-Sutcliffe model efficiency index.

3.2.1. Results

The modelling results for three events, together with measured rainfall and observed discharges are shown in Fig. 13 and Table 2.

Simulation results show a reasonable capture of both the peak flow discharge and the timing of the hydrograph. In several aspects, the proposed method lacks detail when compared to the fully spatial simulations. In particular the width of the hydrograph is not predicted accurately in each event. Such difficulties were similarly found with a full spatially-distributed hydrological model (Hessel et al., 2003b). As
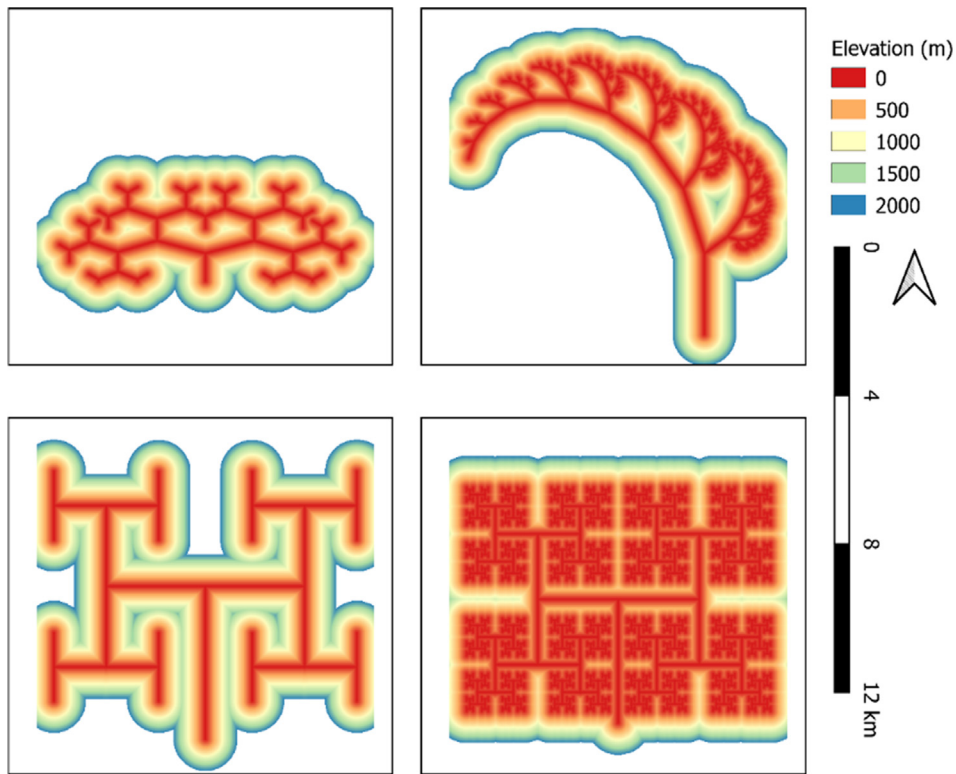
Table 1
A list of require input parameters for the model.

Input Parameter	Note
Slope (spatial)	Classified, parameter 1
Mannings surface roughness (spatial)	Classified, parameter 2
Saturated conductivity (spatial)	Classified, parameter 3
Initial moisture content (non-spatial)	Not classified
Saturation moisture content (non-spatial)	Not classified
Matrix Suction (non-spatial)	Not classified
Elevation (spatial)	Used to estimate the drainage network, inter-slope probability matrix, outflow probabilities and the parameters for the distance-outflow probability density function: D_σ and D_{av}
Precipitation (non-spatial)	Time-dependent graph of rainfall intensity

Fig. 9. Several example catchments created from a fractal-like tree with varying asymmetric and symmetric angles and branch levels. Elevation is based on distance from the network.
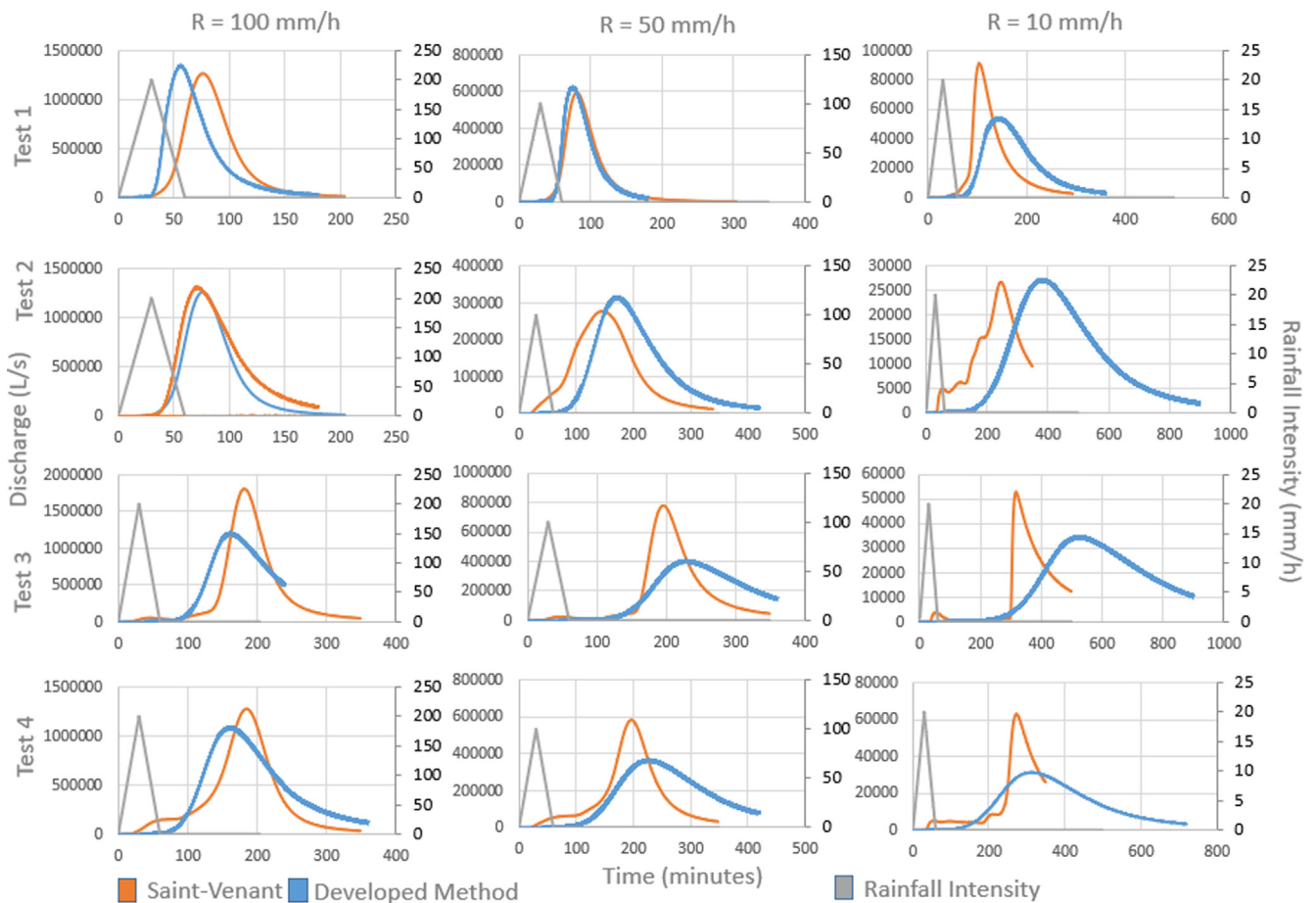

Fig. 10. Uncalibrated simulations of discharge using a variety of rainfall events for the hypothetical catchments.
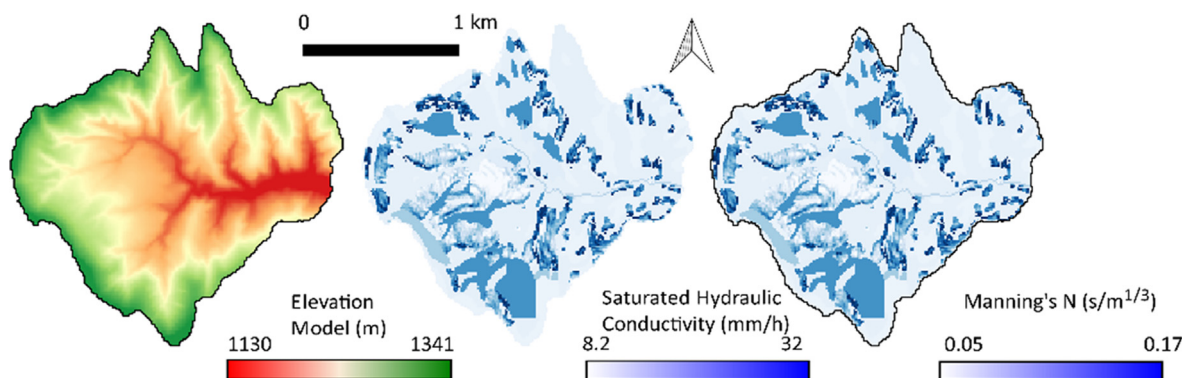
Fig. 11. Maps showing the most relevant physical properties of the Danangau catchment.

proposed by these authors, there are strong non-linear effects induced by the abrupt initiation of runoff after saturation of the top soil layer. This complicates the correct estimation of the initial flow moment. Additionally, the terrain is rough, with steep gullies and sloping farmlands. This complicates accurately representing flow routing within a model, as small and steep elevation patterns predominantly determine the hydrograph dynamics. Most notable to the found results is the accuracy which is comparable to these full spatial simulations while reducing the computational and data requirements significantly.

3.3. Comparison to rational method

To further investigate the implications of the proposed method, we apply a set of synthetic triangular rainfall events with increasing total rainfall depth to both the Prado and Danandau catchments. The precipitation graph is constructed as a triangle with duration of one hour and peak rainfall intensity between 10 and 100 mm/hour with increments of 10 mm/hour. This is then compared with results for peak flow from the rational method. Since the rational method split incoming precipitation into infiltration and runoff based on a constant runoff coefficient, we employ this identical technique for the presented method. For a consistent comparison, we use the same runoff coefficient to simulate infiltration and storage in both methods, which is set

to be 0.3 (typical value, see Thompson, 2006). This value is chosen to indicate the difference between the models in typical scenarios, and does not necessarily represent a calibrated parameter for the Prado area. The results are shown in Fig. 14.

Results from the simulations show the resulted increase in peak flow related to rainfall intensity in both models. The rational method increases linearly. The simplicity of this method results in an unrealistic increase in peak discharge with large rainfall values. However, usage of the method is common in engineering practice due to the simplicity of the method. Peak discharges for the presented methodology do not increase linearly. Instead, the flow method provides a more physically-based estimation of flow dynamics. This includes the increase in flow velocity with increased water height. Because of this, both the peak discharge, timing of the peak and the shape of the hydrograph are altered. This large observed differences can be explained by the assumption of steady-state flow in the rational method. Steady states take significant amounts of time to occur in larger areas. Before this time has passed, the rainfall intensity has changes or the event has passed altogether, such as is the case in the simulations.

3.4. Sensitivity analysis

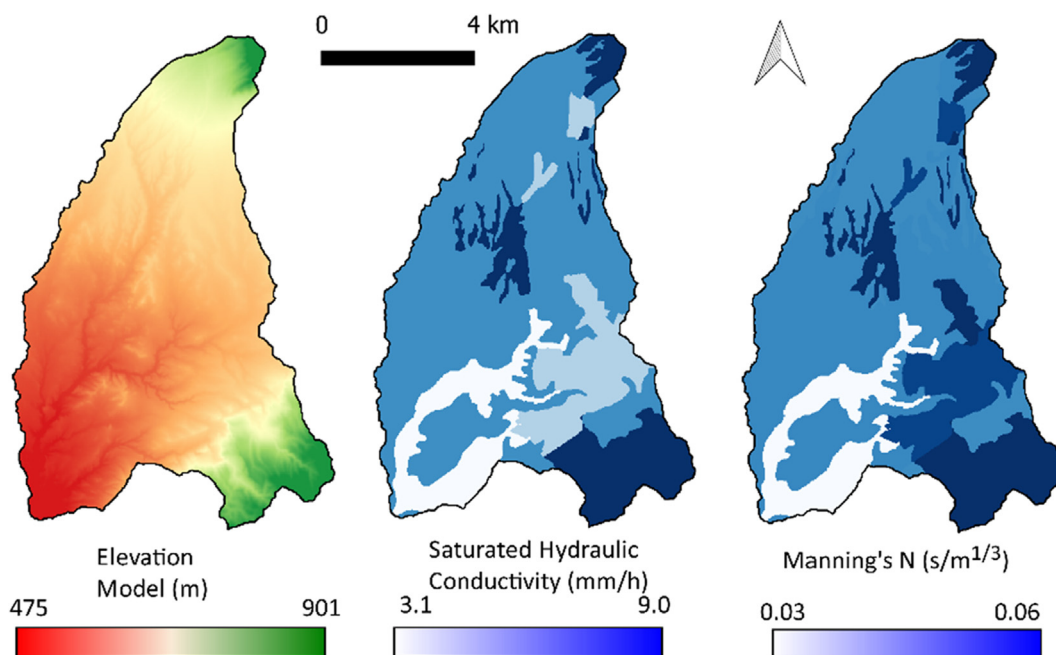Finally, a sensitivity analysis is performed to investigate the

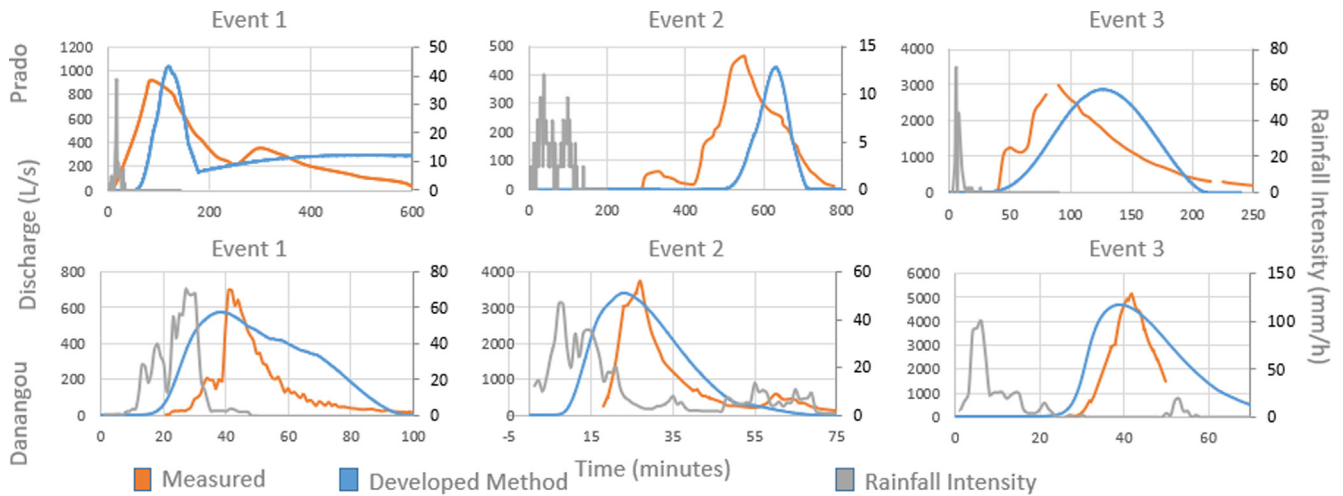**Fig. 12.** Maps showing the most relevant physical properties of the Prado catchment.

Fig. 13. The simulated, calibrated events for both the Prado and Danandou areas.

Table 2
Calibrated parameters and model accuracy for both the Prado and Danandou areas.

	Prado			Danandou		
	K_s	n	NSE	K_s	n	NSE
Event 1	0.71	1.43	0.76	0.67	0.82	0.37
Event 2	0.82	1.19	0.48	0.62	1.32	0.49
Event 3	0.69	1.02	0.65	1.32	0.57	0.62

influence of parameter variability on outflow dynamics. The first event for the Prado Catchment is simulated with limited parameter variability. Three additional simulations with averaged Slope, Ksat and Mannings N are performed respectively (Fig. 15). The results are compared to the simulation with full parameter variability.

As is visible from Fig. 15, differences when using averaged parameter values are significant, altering the peak, total and timing of the discharge. Our semi-spatial terrain description provides interactions between processes that would be seen in full-spatial modelling and reality. Here, this is exemplified by the changes in hydrograph shape resulting from altering a single parameters. Alterations in K_{sat} alter flow height, and therefore flow velocity and thus not only alter peak flow, but timing as well.

We further show the behavior of the proposed methodology by performing a simple sensitivity analysis for the simulations on the Danandou catchment. Here, a triangular rainfall with an averaged intensity of 50 mm/h is taken as input, together with the reference infiltration capacity and manning's N values. Then, both of these inputs are altered by a multiplier ranging between 0.15 and 1.5. The resulting hydrographs are shown in Fig. 16.
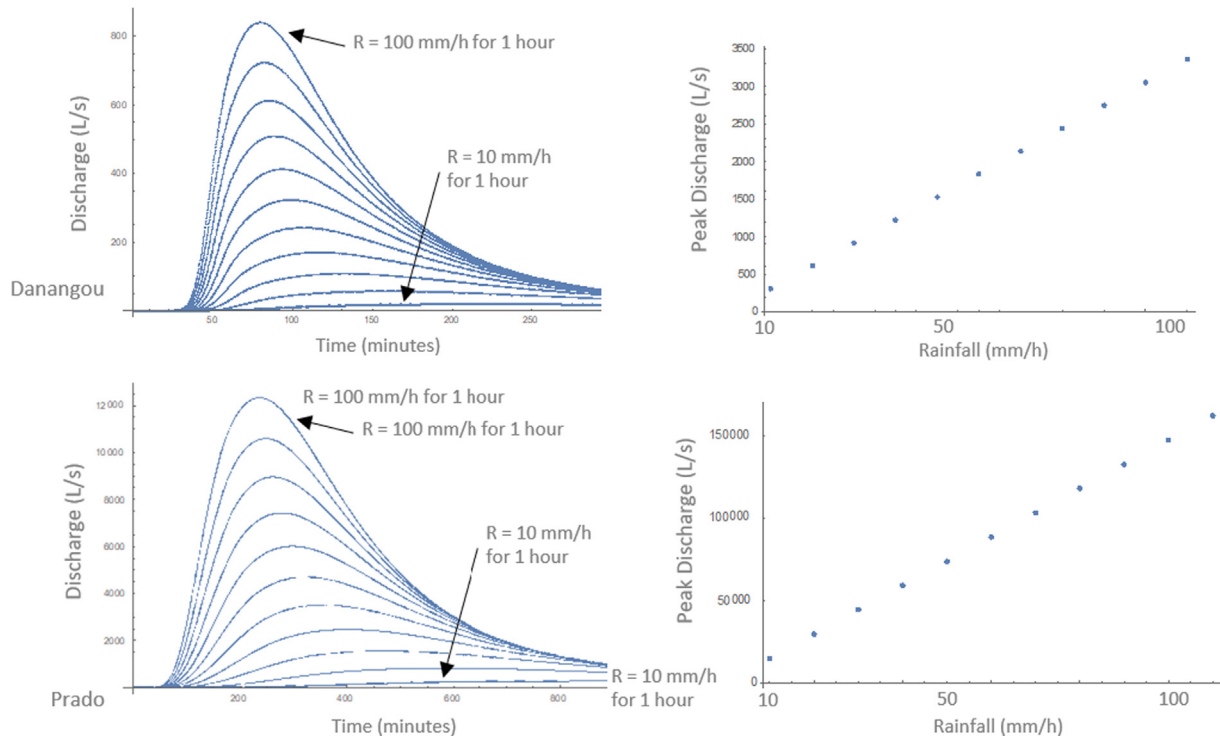

Fig. 14. Simulations results for the Prado and Danandou areas using artificial increasing rainfall. On the right, predicted peak flow using the rational method is provided.
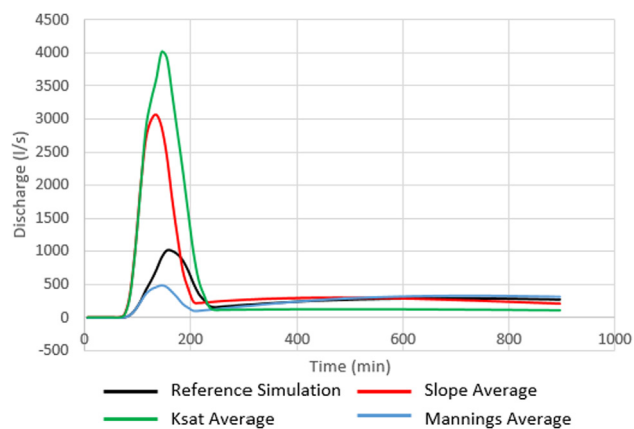
Fig. 15. Simulations results for the Prado event, compared with results using averaged parameters.

The results from the sensitivity analysis show patterns highly similar to the results found in case of full spatial flow and infiltration modelling (Singh, 1997; Pokhrel and Gupta, 2011). The increase of Mannings roughness coefficient decreased flow velocities and thereby delays and lowers the peak outflow value. The delay is visible on the full hydrograph as resulting in a wider and lower shape. For the saturated conductivity, the total outflow volume is directly related to the value of the saturated conductivity of the soils. While lower outflow delays flow velocities and thus delays the peak outflow time, the effect is substantially less significant when compared to the delay from increased values of Mannings N.

4. Future scope of the research

The presented framework for multi-parameter inter-variable catchment hydrology can represent precipitation, flow and infiltration in a semi-spatial manner. The implementation of physically-based equations results in emergent behavior that captures real observations. Alteration of a single input parameter can have consequences for the full dynamics of the model through interactions in the equations and the distributions of water on the terrain. Such behavior is generally found in spatially-distributed physically based models, but lacks in non-spatial empirical models.

The developed framework might, with relative ease, be extended with additional processes to provide a more complete description of full hydrology. For ground water dynamics, the flow scheme as used in surface flow can be adapted by using a depth-averaged Darcy approximation for a saturated ground water layer. Evapotranspiration could similarly be implemented for combinations of land use and soil type.

Finally, a surface storage component could be implemented to capture the storage of water in surface micro-roughness.

Several issues related to the application of the method remain to be investigated. First, the propagation of uncertainty in model input to model outcomes might be investigated. Input parameter uncertainty can complicate usage of model outcomes in decision making as results are less reliable. Ensemble simulations using the proposed method might be investigated to ensure uncertainties are not propagated unnaturally by either the flow scheme or the terrain description. Finally, the multi-parameter inter-variable terrain description can be used to redistribute water into the original terrain. While this could be used for additional modelling steps or visualization, it has to be investigated to what extent this results in realistic outputs. While the semi-spatial terrain description describes the physical processes with good accuracy, this does not necessarily guarantee the internal water distributions represent realistic behavior.

5. Conclusions

We have proposed a new method for estimation of catchment hydrographs using non-spatial physically-based modelling. Our method utilizes a multi-parameter inter-variable statistical catchment description and distributes water over classified physical parameters. Then, a semi-spatial flow scheme is combined with a statistical distribution of the distance to outlet' to calculate an effective probability of outflow for any water. Based on this and rainfall input, a final hydrograph is simulated. The method combines existing physically-based equations for hydrology and flow with a novel semi-spatial HRU scheme. Infiltration can be included in a variety of manners, such as using a runoff coefficient, or the Green and Ampt model. Other processes that can theoretically be included are evapotranspiration, leaf storage and erosion. Finally, using a similar setup for semi-spatial flow, ground water movement could be estimated.

Simulation and calibration results show the method performs well in predicting both uncalibrated and calibrated discharge. In particular, it is able to predict hydrograph peak flows and their time of occurrence with significant accuracy for both for real and hypothetical catchments. The proposed method shows similar sensitivities to full spatial models and allows for calibration and validation. The implementation of non-averaged physical parameters add significant changes to the simulation output, and allows for complex interactions in simulated physical processes. The method could potentially be implemented in global hydrological simulations, allowing for a full global physically-based simulations of hydrology and related processes.

CRediT authorship contribution statement

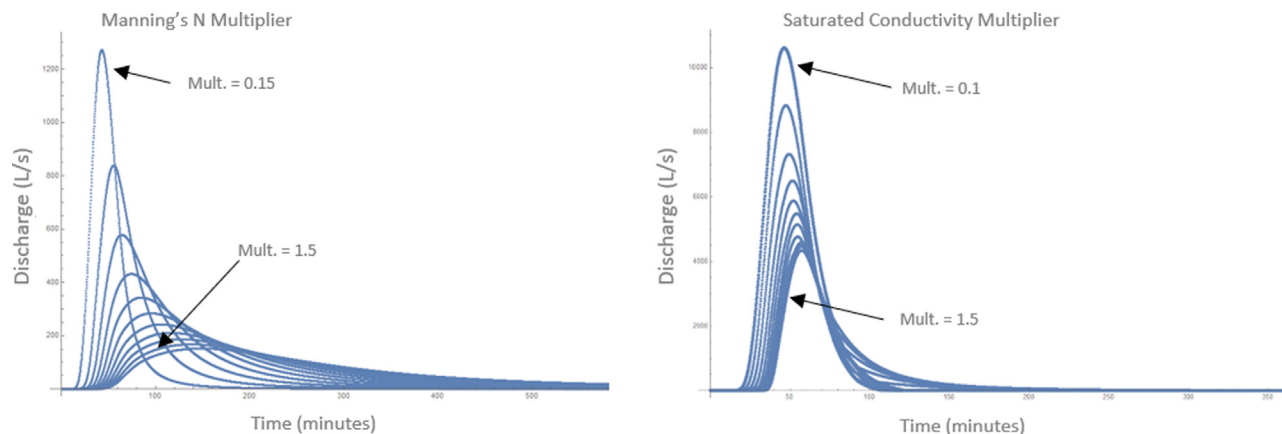**B. Bout:** Conceptualization, visualization, formal analysis, writing

Fig. 16. Sensitivity analysis results for the Danandou catchments. Left: Manning's N is varied. Right: Saturated conductivity is varied.

-original draft. **V. Jetten:** Conceptualization, Writing -review & editing.

interests or personal relationships that could have appeared to influence the work reported in this paper.
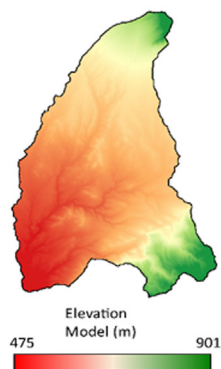
Declaration of Competing Interest

The authors declare that they have no known competing financial

Appendix A. Inter-Slope probability matrices for study areas

A.1: Hypothetical generated catchments, their slope inter-class probabilities and distance distribution
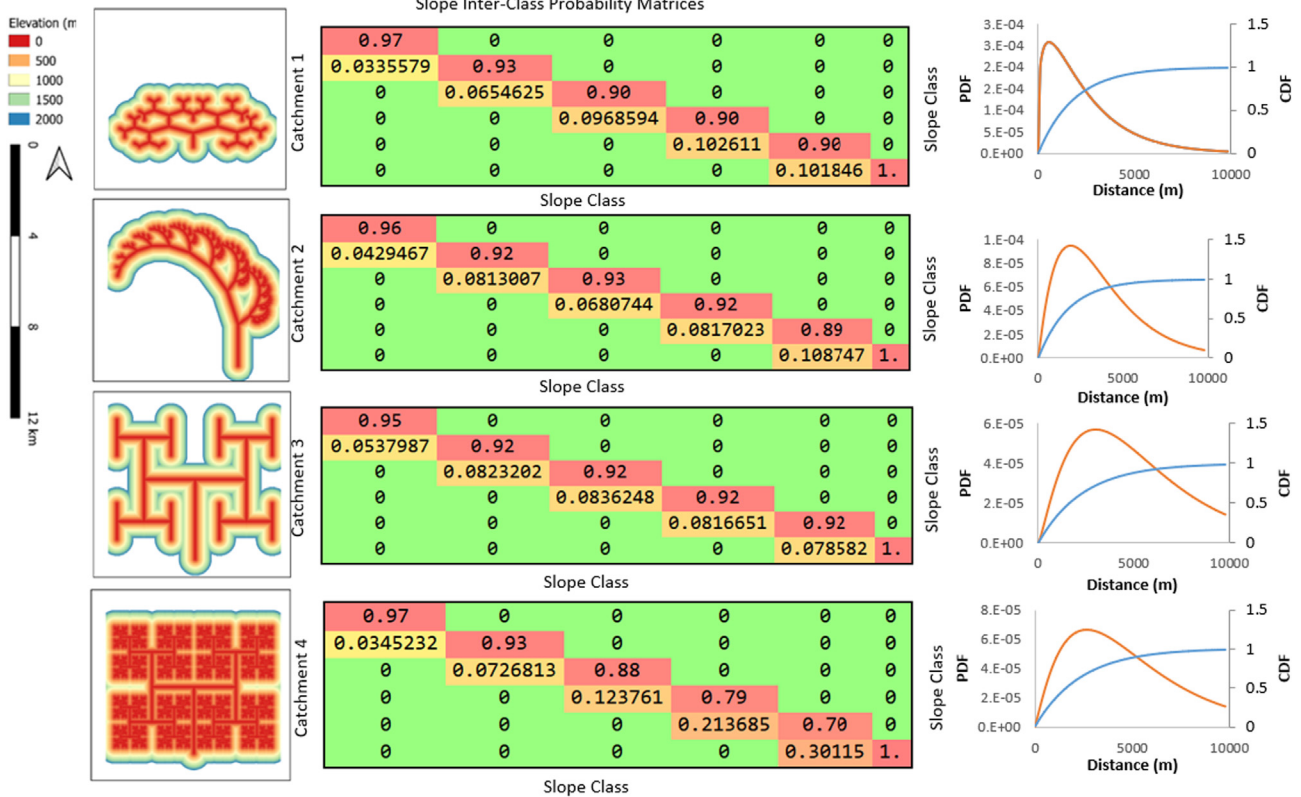
A.2: Study catchments, their slope inter-class probabilities and distance distribution
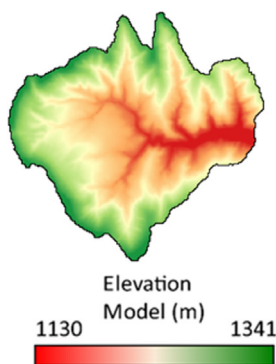
Slope Inter-Class Probability Matrix

0.72	0.12	0.017	0.0055	0.0027	0.00098
0.22	0.57	0.19	0.055	0.023	0.013
0.033	0.21	0.49	0.19	0.051	0.025
0.011	0.059	0.22	0.50	0.19	0.053
0.0066	0.028	0.065	0.21	0.57	0.21
0.0032	0.014	0.023	0.040	0.17	0.70

Slope Inter-Class Probability Matrix

0.76	0.12	0.0055	0	0	0
0.20	0.70	0.22	0.021	0.00050	0
0.032	0.14	0.61	0.26	0.015	0.00051
0.0023	0.032	0.14	0.58	0.19	0.011
0	0.0049	0.019	0.13	0.67	0.21
0	0.00044	0.0025	0.015	0.12	0.78

References

Arnold, J.G., Moriasi, D.N., Gassman, P.W., Abbaspour, K.C., White, M.J., Srinivasan, R., Kannan, N., 2012. SWAT: Model use, calibration, and validation. Trans. ASABE 55 (4), 1491–1508.

Bierkens, M.F., Bell, V.A., Burek, P., Chaney, N., Condon, L.E., David, C.H., Flörke, M., 2015. Hyper-resolution global hydrological modelling: what is next? "Everywhere and locally relevant. Hydrol. Process. 29 (2), 310–320.

Bout, B., Jetten, V.G., 2018. The validity of flow approximations when simulating catchment-integrated flash floods. J. Hydrol. 556, 674–688.

Crawford, N.H., Linsley, R.K., 1966. Digital Simulation in Hydrology'Stanford. Watershed Model 4.

de Graaf, I.D., Sutanudjaja, E.H., Van Beek, L.P.H., Bierkens, M.F.P., 2015. A high-re-solution global-scale groundwater model. Hydrol. Earth Syst. Sci. 19 (2), 823–837.

Dümenil, L., Todini, E., 1992. A rainfall-runoff scheme for use in the Hamburg climate model. In *Advances in theoretical hydrology: a tribute to James Dooge*. Elsevier Science Publishers BV, pp. 129–157.

W.A. Flügel Delineating hydrological response units by geographical information system analyses for regional hydrological modelling using PRMS/MMS in the drainage basin of the River Bröl Germany. Hydrological Processes 9 3–4 1995 423 436.

Foroud, N., 1978. *A flood hydrograph simulation model for watersheds in southern Quebec* (Doctoral dissertation. McGill University).

S. Hagemann L.D. Gates Improving a subgrid runoff parameterization scheme for climate models by the use of high resolution data derived from satellite observations Climate Dynamics 21 3–4 2003 349 359.

Hayes, D. C., & Young, R. L. (2006). Comparison of peak discharge and runoff char-acteristic estimates from the rational method to field observations for small basins in central Virginia(No. 2005-5254).

Green, W.H., Ampt, G.A., 1911. Studies on Soil Phyics. J. Agric. Sci. 4 (1), 1–24.

Hessel, R., Jetten, V., 2007. Suitability of transport equations in modelling soil erosion for a small Loess Plateau catchment. Eng. Geol. 91 (1), 56–71.

Hirabayashi, Y., Mahendran, R., Koirala, S., Konoshima, L., Yamazaki, D., Watanabe, S., Kanae, S., 2013. Global flood risk under climate change. Nat. Clim. Change 3 (9), 816.

James, D. (1970). An Evaluation of Relationships Between Streamflow Patterns and Watershed Characteristics Through the Use of OPSET: A Self Calibrating Version of the Stanford Watershed Model.

Kuichling, E., 1889. The relation between the rainfall and the discharge of sewers in populous districts. Trans. Am. Soc. Civil Eng. 20 (1), 1–56.

López, J.J., Gimena, F.N., Goni, M., Agirre, U., 2005. Analysis of a unit hydrograph model based on watershed geomorphology represented as a cascade of reservoirs. Agric. Water Manag. 77 (1–3), 128–143.

Maidment, D. R. (1993). Handbook of hydrology (Vol. 9780070, p. 397323). New York: McGraw-Hill.

Mishra, S. K., Tyagi, J. V., & Singh, V. P. (2003). Comparison of infiltration models. Hydrological processes, 17(13), 2629-2652.

Morgan, R.P.C., 2001. A simple approach to soil loss prediction: a revised Morgan–Morgan–Finney model. Catena 44 (4), 305–322.

Morgan, R. P. C., & Duzant, J. H. (2008). Modified MMF (Morgan–Morgan–Finney) model for evaluating effects of crops and vegetation cover on soil erosion. Earth Surface Processes and Landforms: The Journal of the British Geomorphological Research Group, 33(1), 90-106.

Pokhrel, P., Gupta, H.V., 2011. On the ability to infer spatial catchment variability using streamflow hydrographs. Water Resour. Res. 47 (8).

Singh, V.P., 1997. Effect of spatial and temporal variability in rainfall and watershed characteristics on stream flow hydrograph. Hydrol. Process. 11 (12), 1649–1669.

Thompson, D. B. (2006). The rational method. David B. Thompson Civil Engineering Department Texas Tech University. pp, 1-7.

Soil Conservation Service, 1972. National engineering handbook, section 4, hydrology. US Department of Agriculture, Washington, DC.

Yamazaki, D., Sato, T., Kanae, S., Hirabayashi, Y., Bates, P.D., 2014. Regional flood dy-namics in a bifurcating mega delta simulated in a global river model. Geophys. Res. Lett. 41 (9), 3127–3135.